



This is a repository copy of *The ultrastructural distribution of prestin in outer hair cells: a post-embedding immunogold investigation of low-frequency and high-frequency regions of the rat cochlea.*

White Rose Research Online URL for this paper:

<https://eprints.whiterose.ac.uk/152634/>

Version: Accepted Version

Article:

Mahendrasingam, S., Beurg, M., Fettiplace, R. et al. (1 more author) (2010) The ultrastructural distribution of prestin in outer hair cells: a post-embedding immunogold investigation of low-frequency and high-frequency regions of the rat cochlea. *European Journal of Neuroscience*, 31 (9). pp. 1595-1605. ISSN 0953-816X

<https://doi.org/10.1111/j.1460-9568.2010.07182.x>

This is the peer reviewed version of the following article: Mahendrasingam, S. , Beurg, M. , Fettiplace, R. and Hackney, C. M. (2010), The ultrastructural distribution of prestin in outer hair cells: a post-embedding immunogold investigation of low-frequency and high-frequency regions of the rat cochlea. *European Journal of Neuroscience*, 31: 1595-1605, which has been published in final form at <https://doi.org/10.1111/j.1460-9568.2010.07182.x>. This article may be used for non-commercial purposes in accordance with Wiley Terms and Conditions for Use of Self-Archived Versions.

Reuse

Items deposited in White Rose Research Online are protected by copyright, with all rights reserved unless indicated otherwise. They may be downloaded and/or printed for private study, or other acts as permitted by national copyright laws. The publisher or other rights holders may allow further reproduction and re-use of the full text version. This is indicated by the licence information on the White Rose Research Online record for the item.

Takedown

If you consider content in White Rose Research Online to be in breach of UK law, please notify us by emailing eprints@whiterose.ac.uk including the URL of the record and the reason for the withdrawal request.



eprints@whiterose.ac.uk
<https://eprints.whiterose.ac.uk/>

Published in final edited form as:

Eur J Neurosci. 2010 May ; 31(9): 1595–1605. doi:10.1111/j.1460-9568.2010.07182.x.

The ultrastructural distribution of prestin in outer hair cells: a post-embedding immunogold investigation of low and high frequency regions of the rat cochlea

Shanthini Mahendrasingam¹, Maryline Beurg², Robert Fettiplace³, and Carole M Hackney⁴

¹School of Life Sciences, Keele University, Keele, UK.

²INSERM U587, Université Victor Segalen Bordeaux 2, Hôpital Pellegrin, Bordeaux, France

³Department of Physiology, University of Wisconsin, Madison

⁴Department of Biomedical Science, University of Sheffield, UK

Abstract

Outer hair cells (OHCs) of the mammalian cochlea besides being sensory receptors also generate force to amplify sound-induced displacements of the basilar membrane thus enhancing auditory sensitivity and frequency selectivity. This force generation is attributable to voltage-dependent contractility of the OHCs underpinned by the motile protein, prestin. Prestin is located in the basolateral wall of OHCs and is thought to alter its conformation in response to changes in membrane potential. The precise ultrastructural distribution of prestin was determined using post-embedding immunogold labelling and the density of the labelling was compared in low and high frequency regions of the cochlea. The labelling was confined to the basolateral plasma membrane in hearing rats but declined towards the base of the cells below the nucleus. In pre-hearing animals, prestin labelling was lower in the membrane and also occurred in the cytoplasm, presumably reflecting its production during development. The densities of labelling in low-frequency and high-frequency regions of the cochlea were similar. Non-linear capacitance, thought to reflect charge movements during conformational changes in prestin, was measured in OHCs in isolated cochlear coils of hearing animals. OHC non-linear capacitance in the same regions assayed in the immunolabelling was also similar in both apex and base, with charge densities of 10,000 / μm^2 expressed relative to the lateral membrane area. The results suggest that prestin density and by implication force production, is similar in low-frequency and high-frequency OHCs.

Keywords

electron microscopy; capacitance measurements; cochlear amplifier; immunocytochemistry

Introduction

The mammalian cochlea contains two types of hair cell, inner hair cells (IHCs) and outer hair cells (OHCs), embedded in a sensory epithelium, the organ of Corti. The organ of Corti sits on the basilar membrane which runs the length of the cochlea and varies in its stiffness

and width from cochlear apex to base. Sound stimuli result in movements of the basilar membrane, low frequencies vibrating the apical region and high frequencies the base (von Békésy, 1960). Sound signals *in vivo* are thought to be enhanced by active mechanisms in OHCs (Dallos, 1992; Fettiplace & Hackney, 2006). Whereas IHCs relay auditory signals via the VIIIth nerve to the brain, OHCs boost the stimulus by electromechanical feedback. This mechanism has been called 'the cochlear amplifier' because it increases both the amplitude and frequency selectivity of basilar-membrane vibrations for low level sounds (Dallos *et al.*, 2006). The prevailing view is that the cochlear amplifier arises from voltage-dependent contractility of the elongated OHCs dependent on a membrane protein, prestin, expressed in OHCs but not IHCs (Zheng *et al.*, 2000; Ashmore, 2008). The importance of prestin has been demonstrated by construction of mutations that abolish its expression (Liberman *et al.*, 2002) or modify its function (Dallos *et al.*, 2008). Such mutations reduce or eradicate OHC somatic electromotility and cochlear sensitivity in tandem without affecting forward mechanical transduction.

An unresolved problem with prestin-mediated somatic motility is that at high frequencies, above 1 kHz, it may be reduced due to attenuation of the driving voltage, the receptor potential, by the OHC time constant (Santos-Sacchi, 1992; Housley & Ashmore, 1992; Preyer *et al.*, 1996). Several solutions have been proposed (e.g., Dallos & Evans, 1995; Weitzel *et al.*, 2003; Rybalchenko & Santos-Sacchi, 2003; Ramamoorthy *et al.*, 2007; Mistrik *et al.*, 2009) but none has been fully confirmed experimentally. To counteract this problem, it is often assumed that high frequency OHCs can produce a much larger force than low frequency OHCs (Geisler, 1993; Lu *et al.*, 2006). In support of the assumption, it has been suggested that OHCs tuned to higher frequencies may have a greater density of prestin than lower frequency cells as indicated by the density of motility-related charges, the non-linear capacitance (Santos-Sacchi *et al.*, 1998). The precise argument depends on knowing the fraction of OHC membrane that contains prestin. Most previous studies used immuno-fluorescence with light microscopy which can neither precisely localize the prestin nor is it fully quantitative. Some have shown a non-uniform sub-cellular distribution of prestin (Belyantseva *et al.*, 2000) but others have concluded it is expressed on the entire basolateral surface of the OHC (Yu *et al.*, 2006). Here, the distribution was examined using post-embedding immunogold labelling of prestin, which permitted quantification of the distribution and density of labelling in OHCs from apical and basal regions of the rat cochlea and comparisons between animals of different ages. Results from immunolabelling were supplemented with independent assay of the prestin density based on measurements of non-linear capacitance in the two cochlear regions.

Materials and methods

Animals and fixation

The methods for tissue fixation and immunolabelling were similar to those described previously (Hackney *et al.*, 2005). Cochleas were obtained from Sprague Dawley rats on postnatal days 7 (P7, pre-hearing) and 16 (P16, post-hearing) using procedures approved by the Animal Care Committee at the University of Wisconsin-Madison and in accordance with the UK Animals (Scientific Procedures) Act 1986. Preyer reflex tests indicated that the P16 animals had acoustic startle responses but the P7 animals did not. For tissue fixation, animals were deeply anaesthetised with ketamine (50–100 mg/kg) and xylazine (4–8 mg/kg) or with pentobarbitone (Pentoject: 100 mg/kg) injected intraperitoneally. After loss of the pedal withdrawal reflex, they were perfused transcardially for 1 min with a vascular flush consisting of buffered saline containing 5% dextran or heparin (7.2 U/ml) and 0.15% procaine HCl and then for 10 min with 4% paraformaldehyde and 0.1% glutaraldehyde in 0.1 M sodium phosphate buffer (PB), pH 7.4. After perfusion, the animals were decapitated, the auditory bullae opened, and each cochlea was fixed further by perfusion of the same

fixative via a small hole made in the cochlear apex and base followed by immersion in the same fixative for 2h at room temperature (20°C).

Electron microscopy and immunogold labelling

Cochlear segments from both apical and basal locations were dissected out and washed in PB and then dehydrated in a graded series of ethanols. The pieces of tissues were infiltrated with LR-White resin (Agar Scientific, Stansted, UK) for 24 h and placed in gelatine capsules and polymerized in fresh resin at 50°C for 24 h. Ultrathin sections were cut on a Leica (Nussloch, Germany) ultramicrotome and collected on 200-mesh nickel grids. For the immunogold labelling procedure, grids containing sections were immersed in a series of droplets of each solution (30 µl) on a strip of Parafilm within a humid chamber. The grids were incubated in 0.05 M Tris-buffered saline (TBS), pH 7.4, and non-specific protein binding was blocked using 20% goat serum and 0.2% Tween 20 in TBS for 30 min at room temperature. They were then incubated overnight at 4°C in primary antibody in 0.05M TBS containing 1% bovine serum albumin and 0.02% Tween 20 (BSA-T20-TBS). An affinity purified rabbit polyclonal antibody to the C-terminal rat prestin peptide sequence TVLPPQEDMEPNATPTTPEA (Bethyl Laboratories Inc, Montgomery, TX) was used at a dilution of 1:25,000 or 1:50,000, the latter dilution being employed for all quantification. These dilutions correspond to absolute antibody concentrations of 0.044 and 0.022 µg/ml respectively. In some experiments an antibody to an N-terminal sequence KYLVERPIFSHPVLQE (also from Bethyl Laboratories) was used at a dilution of 1:100, equivalent to a concentration of 10 µg/ml. After treatment with primary antibody, grids were washed in BSA-T20-TBS and incubated in goat anti-rabbit IgG conjugated to 15 nm gold particles (British BioCell, Cardiff, UK) diluted 1:20 in BSA-T20-TBS for 2 h at room temperature. The grids were washed again in TBS and distilled water, stained in aqueous uranyl acetate for 20 min and examined using a JEOL JEM 1230 transmission electron microscope operated at 100kV. For a negative control, grids containing sections were incubated in BSA-T20-TBS without the primary antibody. No labelling was ever observed.

Immunoblots—Four rats were anaesthetised with sodium pentobarbital (i.p., 100 mg/kg Pentoject, Animal Care, York, UK), bullae removed, and the organs of Corti were stripped in 20 mM phosphate buffer containing 5 mM ethylene diaminetetraacetic acid (EDTA). Tissues collected from the four animals were transferred into 20 µl of 0.02M PB with 5 mM EDTA and 1 mM phenylmethylsulphonyl fluoride (PMSF) and boiled with 20 µl of sample buffer (0.0625 M Trizma-HCl, pH 6.5 containing 2% sodium dodecyl sulphate (SDS), 5% mercaptoethanol, 10% glycerol and 0.001% bromophenol blue) for 3 min at 100°C, proteins separated on a 10% polyacrylamide gel and blotted onto nitrocellulose. Blots were incubated with anti-prestin C-terminal antibody diluted 1:25,000 or N-terminal antibody diluted 1:100 in dilution buffer (0.05 M Tris-buffered saline containing 2% goat serum and 0.2% Tween 20) and visualized using the biotin extravidin-peroxidase (Sigma, UK). Immunoblots of rat organ of Corti showed a principal band at approximately 80 kDa when labelled with either the C-terminal or N-terminal antibody suggesting that a single isoform of prestin molecule is present in the cochlea (Fig. 1). The predominant form of rat prestin is expected to have molecular mass of 81.4 kDa. There was no evidence for significant occurrence of shorter isoforms reflecting the truncated C terminus variants such as SLC26A5d (with 40 kDa molecular mass) described in the human genome (Liu *et al.*, 2003). These variants should have been labelled with the N-terminal but not the C-terminal antibody. There was, however, a higher molecular weight band at ~112 kDa. This band was at too small a molecular weight to be a prestin dimer but may correspond to a glycosylated form of prestin as reported previously (Matsuda *et al.*, 2004).

To localize precisely the distribution of prestin along the basolateral wall of OHCs (Fig 6), one Sprague Dawley P16 rat was fixed in the same way and cochlear segments were dissected and cryoprotected by immersion in increasing concentration of glycerol in PB (10, 20, 30 %). They were then plunge frozen in liquid propane, immersed in anhydrous methanol containing 0.5% uranyl acetate at -85°C , brought gradually up to -45°C , rinsed in methanol and infiltrated with increasing concentrations of Lowicryl HM20 resin and polymerised in pure resin with UV light. The reason for using glycerol and embedding in HM 20 resin was to enhance membrane preservation in the hearing animal so that the precise localization of prestin with respect to the plasma membrane could be demonstrated. Ultrathin sections were cut and labelling was carried out using antibodies to rabbit polyclonal anti-prestin C- and N-terminals diluted 1:25,000 and 1:100 respectively and goat anti-rabbit IgG conjugated to 5 nm gold particles diluted 1:20 in BSA-T20-TBS.

Semi-quantitative analysis of immunogold labelling

The density of gold labelling was determined in radial sections of the cochleas taken from an apical coil (low frequency region), and a basal coil (high frequency region) of P7 and P16 rats. This labelling density has been defined as 'semi-quantitative' because, although it represents a comparison of the relative densities of prestin, it does not indicate the absolute amount of prestin present in the membrane. Grids containing sections from apical and basal location of the cochlea were placed in the same drops of solution and sections from P7 and P16 rats were incubated in the same batch of solutions, and immunogold labelling was performed simultaneously. To count the number of gold particles along the basolateral wall of OHCs, micrographs of OHCs from different rows (the OHC closest to the outer pillar cell is referred to as OHC1, the OHC in the middle as OHC2, and the OHC furthest away from the outer pillar cell as OHC3) were taken at the same magnification (15,000 X or 50,000 X). Gold particles on either side of the basolateral wall (within the spatial resolution distance of 24 nm from the epitopic binding site to the middle of the gold particle) were counted along every micrometer (1 μm), starting from the base of the tight junction on the *stria vascularis* side and ending at the base of the tight junction on the modiolar side of the hair cell. When an entire length of a hair cell was not in the radial section plane (some regions lay in a tangential section plane), gold particles on either side of the basolateral wall within the spatial resolution distance of 24 nm were counted along every micrometer, starting from the base of junction on the *stria vascularis* side and from the base of junction on the modiolar side to whatever length that was possible in the radial section plane. Graphs were plotted using a moving average (per 5 μm) to investigate the trend of prestin labelling along the basolateral wall of OHC from P7 and P16 rats in apical and basal locations. To plot the graphs using moving average on the ordinate, the average number of gold particles within 1–5 μm , 2–6 μm , 3–7 μm , 4–8 μm and so on was calculated.

Non-linear capacitance

Experiments were performed on OHCs in isolated temporal bones of P14 – P18 Sprague-Dawley rats with techniques reported previously (Kennedy *et al.*, 2003). Animals were anesthetized with halothane and killed by decapitation using methods approved by the Institutional Animal Care and Use Committee of the University of Wisconsin-Madison and in accordance with NIH guidelines. An excised piece of temporal bone was immobilized in a thin slice of silastic tubing (~3 mm internal diameter) glued to a plastic cover slip and the cochlea was exposed by removing the bone and lifting off the tectorial membrane. The cover slip and preparation were then transferred to the experimental chamber and viewed through a 40X long working distance water-immersion objective (numerical aperture = 0.8) on a Zeiss Axioskop FS microscope. The chamber was perfused with artificial perilymph of composition (in mM): 154 NaCl, 6 KCl, 1.5 CaCl₂, 2 Na-pyruvate, 8 glucose and 10 Na-HEPES, pH 7.4. To block fully voltage-sensitive K⁺ conductances, 10 mM tetraethyl

ammonium Cl (TEA) and 30 μ M 10,10-bis(4-pyridinylmethyl)-9(10H)-anthracenone dihydrochloride (XE991; Tocris Bioscience, Ellisville, Missouri), a selective inhibitor of KCNQ K⁺ channels (Robbins, 2001), was added to the artificial perilymph. Whole cell recordings were performed at room temperature (21 – 23 °C) with borosilicate patch electrodes connected to an Axopatch 200A amplifier. Patch pipettes were filled with an intracellular solution of composition (in mM): 135 CsCl, 2 MgCl₂, 1 EGTA, 3 Na₂ATP, 0.5 Na₂GTP, 10 creatine phosphate and 10 CsHEPES pH 7.2. Patch pipettes had starting resistances of 3 – 6 M Ω . Membrane currents were low-pass filtered at the output of the Axopatch 200A amplifier at 10 kHz. Membrane potentials were corrected for a 4 mV liquid junction potential. Recordings were made from first or second row OHCs either at the beginning of the apical turn, about 0.8 of the distance along the basilar membrane, or in the basal turn 0.3 of the distance from the round window. From the place-frequency map in adult rats, the recording sites correspond to characteristic frequencies of approximately 4 kHz and 30 kHz respectively (Müller, 1991). In some experiments, OHCs were detached from the organ of Corti in order to determine their dimensions.

A continuous measurement of OHC membrane capacitance was obtained as previously described (Santos-Sacchi *et al.*, 1998b) by delivering a voltage clamp protocol consisting of either a single sine wave (10 mV peak-to-peak at 391 Hz) or a double sine wave (10 mV peak-to-peak at 391 Hz and at 781 Hz). The sine waves were superimposed on a 200 ms voltage ramp from –150 to +150 mV. Voltage commands and data acquisition were performed with a Windows-based patch-clamp program jClamp (www.SciSoftCo.com) using a Micro1401 Interface (CED, Cambridge UK). Membrane potentials were corrected for series resistance off line. The membrane capacitance C_m was derived by admittance analysis assuming a three component network comprising membrane capacitance and resistance in series with access resistance (Gillis, 1995). This was implemented in jClamp and the variation of C_m with membrane potential, V_m , was fitted with the first derivative of a two-state Boltzmann function (Santos-Sacchi *et al.*, 1998b):

$$C_m = Q_{\max} \frac{ze}{kT} \frac{\varepsilon}{(1+\varepsilon)^2} + C_{LIN} \quad (1)$$

where

$$\varepsilon = \exp\left(\frac{ze(V_m - V_{0.5})}{kT}\right) \quad (2)$$

The fits enabled evaluation of the Boltzmann parameters: Q_{\max} (the maximum nonlinear charge moved), $V_{0.5}$ (the voltage at peak capacitance), z (the valence) and C_{LIN} (the linear membrane capacitance). e is the electronic charge, k is the Boltzmann constant and T is absolute temperature. The linear capacitance C_{LIN} is the minimum capacitance that was obtained from the fit at depolarized membrane potentials.

Statistical analysis

The results are presented as the mean \pm either 1 standard deviation (SD) or 1 standard error of the mean (SEM) as indicated. For the electron microscopic data, statistical significance between means was assessed with a non-parametric test (Wilcoxon signed rank sum test, also known as the Mann-Whitney U -test) because of the distribution of data points. The physiological data were compared using the Student's t -test (two-tailed).

Results

Prestin labelling in pre-hearing animals

In pre-hearing (P7) rats, immunogold labelling using the C-terminus antibody for prestin was localized on the basolateral wall and in the cytoplasm of OHCs but not in any other subcellular compartments (Fig. 2), and in hearing (P16) rats it was localized only on the basolateral wall of OHCs (Fig. 4). As expected from previous work (Zheng et al., 2000; Belyantseva *et al.*, 2000), IHCs were not labelled (Fig. 4C). In P7 rats, the basolateral wall of apical OHCs was more heavily labelled for prestin than the basolateral wall of the basal ones (Fig. 2), and semi-quantitative analysis indicated the same trend (Fig. 3). The moving average trends for the apical OHCs were different from those of the basal ones because the apical OHCs were longer than the basal ones. The mean densities of gold labelling for prestin in the apical ($n = 51$) and basal ($n = 28$) OHC1 (see e.g., Fig. 3A) were counted in 1- μm lengths and were $1.73 \mu\text{m}^{-1} \pm 0.22$ (SEM) and $0.68 \mu\text{m}^{-1} \pm 0.17$ (SEM) respectively and the difference was significant ($P = 0.001$). For apical ($n = 36$) and basal OHC3 ($n = 24$) (Fig. 3B), the densities were $2.06 \mu\text{m}^{-1} \pm 0.30$ (SEM) and $0.75 \mu\text{m}^{-1} \pm 0.20$ (SEM) respectively and again the difference was significant ($P = 0.002$). A total of four OHCs were quantified and the density of labelling for prestin in the apical OHC1 and OHC3 was not significant ($P = 0.54$) and the same was true for the basal OHC1 and OHC3 ($P = 0.77$). The basolateral walls, including the nuclear zone and the region below it were labelled for prestin in both apical and basal OHCs. The cytoplasm below the cuticular plate and below the nucleus of both apical and basal OHCs was also labelled for prestin. Qualitatively and semi-quantitatively, no obvious difference was observed in the labelling density between the basolateral walls of the first and third rows of OHCs in either the apical or basal regions.

Prestin labelling in hearing animals

In P16 rats, there was little or no label in the cytoplasm and the label was confined to the basolateral walls above the nucleus of OHCs from both apical and basal locations and showed similar densities of labelling for prestin (Figs. 4A and 4B). The basolateral walls of OHCs from the apical location had less labelling in the subnuclear region (Fig. 5A) compared to that of the supranuclear region (Fig. 4A) and very few or no gold particles were present in the region where the nerve terminals form contacts with the OHCs (Fig. 5A). In comparison, the basolateral wall of the basal OHCs showed reduced labelling at the level of the nucleus but very few or no gold particles were seen in the subnuclear region and in the region where the nerve terminal and Deiters' cells forms contacts with the OHCs (Fig. 5B). To establish more accurately the location of the prestin, some sections were labelled with smaller 5 nm gold particles (see Methods) using both N-terminal and C-terminal antibodies (Fig. 6). These results demonstrated that the label was confined to the lateral membrane and not present in the submembranous cisternae. Although the apical OHCs are longer than the basal OHCs, the moving average trends for the apical and basal OHCs displayed a similar pattern (Fig. 7) and the labelling above the nucleus of both apical and basal OHCs was not significantly different from each other ($P = 0.34$). Both indicate a plateau in prestin labelling above the nucleus but a sudden decrease in labelling at the level of nucleus. The basolateral wall above the nucleus of an apical OHC1 from a P16 rat was more heavily labelled for prestin than an OHC1 from a P7 rat, and both moving average trends and semiquantitative analysis indicated that the same region of OHC1 from the P16 rat was five to ten times more heavily labelled than the one from the P7 rat.

In addition to the moving averages, counts of gold particles were made on a number of cells in the supranuclear region where the labelling density appears constant (Table 1). No obvious difference in the intensity of labelling for prestin was evident between OHC1,

OHC2 and OHC3 from the same location and therefore the counts were pooled for each cochlear location. Including all three rows of OHCs, the mean counts were 21.9 ± 2.6 (SD) particles μm^{-1} in 11 OHCs from the apex and 23.4 ± 3.8 (SD) particles μm^{-1} in 14 cells from the base. The results indicate no significant difference between the two cochlear locations (Table 1, $P > 0.05$). Owing to the high densities of labelling on the basolateral wall in the P16 animals, it is conceivable that saturation of labelling or occlusion of neighbouring epitopic sites might have masked differences between apex and base. To examine this problem, comparison was made of counts in P16 animals using the lower efficiency antibody to the prestin N-terminus. Mean counts of OHCs from all three rows (\pm SD) were $2.00 \pm 0.60 \mu\text{m}^{-1}$ ($n = 14$, apex) and $2.43 \pm 1.11 \mu\text{m}^{-1}$ ($n = 11$, base). These values are not significantly different ($P > 0.05$). However, it should be noted that these are linear densities and the ratio of a real densities between basal and apical locations could be $(2.43/2.00)^2$, which is about a factor of 1.5

Non-linear capacitance

Non-linear capacitance measurements were used to infer the characteristics of the gating charge movements (Table 2, Fig. 8B) thought to be dominated by the voltage-dependent activation of prestin (Santos-Sacchi, 1991; Tunstall *et al.*, 1995). To ensure that the capacitance measurements were not distorted by the presence of a significant membrane conductance, the predominant voltage dependent K^+ channels were blocked by intracellular Cs^+ and 10 mM TEA. Although these agents were sufficient to produce a high resistance membrane in apical OHCs, this was not the case in the basal OHCs which possess a large $G_{\text{K,n}}$ conductance (Mammano & Ashmore, 1996) flowing through KCNQ4 channels active at negative potentials. However, both inward and residual outward currents attributable to this channel were abolished by 30 μM XE991 (Fig. 8A), a specific inhibitor of KCNQ channels (Robbins 2001). For apical OHCs of P16 – P18 hearing rats, in which prestin expression and function are close to those achieved in the adult (Belyantseva *et al.*, 2000), the Boltzmann fits had a half-activation membrane potential of -38 ± 3 mV and valence of 0.95 ± 0.05 (SD; $n = 35$). These values closely match the equivalent parameters for voltage-dependent contractions of OHCs isolated from animals of the same age range (-47 mV and 0.9 respectively for cells with a mean length of 33 μm ; Kennedy *et al.*, 2006). Corresponding measurements from the basal turn in the same age range gave very similar values for both half-activation membrane potential (-42 ± 3 mV) and valence (0.91 ± 0.07 (SD), $n = 11$). The maximum charge transfers in apex and base, when normalized to the total OHC membrane area, yielded charge densities of $6,987 \pm 559$ (SD) $\text{e}^- \mu\text{m}^{-2}$ (apex) and 6146 ± 926 (SD) $\text{e}^- \mu\text{m}^{-2}$ (base). The values for charge density are similar to those reported by others for rat apical OHCs ($\sim 7200 \text{e}^- \mu\text{m}^{-2}$ in isolated cells of adults; Belyantseva *et al.*, 2000; $\sim 4400 \text{e}^- \mu\text{m}^{-2}$ in P14 animals inferred from data of Oliver & Fakler, 1999). The half-activation voltages, $V_{0.5}$, are also comparable to those reported in previous measurements on rat OHCs (e.g., $V_{0.5} \sim -40$ mV in isolated cochlear coils of P14 rats; Fig. 3B, Oliver & Fakler, 1999). There is evidence that the prestin charge density increases with development (Oliver & Fakler 1999; Belyantseva *et al.*, 2000) with the apical region lagging the base by two days. The apical mean charge densities (\pm SD) measured for P16 – P18 rats ($6,987 \pm 559 \text{e}^- \mu\text{m}^{-2}$; $n = 35$) and in P14 – P15 rats ($6849 \pm 668 \text{e}^- \mu\text{m}^{-2}$; $n = 12$) do not differ significantly ($P > 0.2$), suggesting that the measured values are close to maximal.

In determining the prestin charge density, the membrane area was inferred from the total linear capacitance assuming a specific membrane capacitance of $0.01 \text{pF} \mu\text{m}^{-2}$ (equivalent to $1 \mu\text{F} \text{cm}^{-2}$). The prestin, however, is confined to the basolateral walls and the local densities will therefore be larger. To correct the charge densities for the non-uniform distribution of prestin, in particular, its absence at the top and bottom of the cell, OHC dimensions were measured in semi-isolated cells from the two cochlear locations. The mean

length, L , and radius, r , of these cylindrical cells (\pm SD) were $39.5 \pm 1.1 \mu\text{m}$ and $4.0 \pm 0.3 \mu\text{m}$ in five apical cells and $18.3 \pm 1.4 \mu\text{m}$ and $3.6 \pm 0.3 \mu\text{m}$ in five basal cells. If it is assumed that prestin is uniformly distributed along the entire lateral wall from tight junction to half-way down the nucleus (i.e., it finishes at a distance r from the bottom of the hair cell but is excluded from the top of the cell including the hair bundle), the membrane area is $2\pi r(L-r)$, which is $892 \mu\text{m}^2$ (apex) and $333 \mu\text{m}^2$ (base). Using these membrane areas, the corrected mean charge densities (\pm SD) become $9473 \pm 758 \text{e}^- \mu\text{m}^{-2}$ (apex; $n = 35$) and $9966 \pm 1466 \text{e}^- \mu\text{m}^{-2}$ (base; $n = 11$), values that are not significantly different ($P > 0.05$).

Discussion

Prestin localisation

Post embedding immunogold labelling for prestin was performed on OHCs from P7 and P16 rats, stages corresponding to an immature and close to a mature level of OHC development and somatic motility (Oliver & Fakler, 1999; Belyantseva *et al.*, 2000). Labelling was confined to the membrane and was seen along virtually the entire basolateral wall of the OHCs. However, it was reduced below the nucleus and the only membrane regions where it was absent were those associated with cellular contact on the efferent nerve terminal and above the base of the tight junction at the cell apex. In pre-hearing rats, prestin labelling was seen in the cytoplasm, presumably because it is being manufactured for insertion into the basolateral wall whereas in hearing rats, little cytoplasmic labelling was seen suggesting a lower turn-over. It is possible that prestin is being inserted at the top of the cell and is moving down towards the base, a potential explanation for the gradient in labelling along the basolateral wall. Further ultrastructural studies with double- or triple-labelling could be used to ascertain the relationship of prestin to the cytoskeletal network (Jensen-Smith & Hallworth, 2007; Legendre *et al.*, 2008) that lies just beneath the plasma membrane.

Prestin density

There was a difference between apical and basal levels of prestin in P7 animals during development but, in P16 hearing animals there was little difference in the density of the labelling for prestin in high and low frequency regions of the cochlea. It is unlikely that this result can be accounted for by steric hindrance because the density of labelling was not sufficiently high for the antibodies and gold particles to be interfering with each other between antigenic sites. Consistent with this idea, observations with a less efficient N-terminal antibody confirmed the small difference between apical and basal locations. These results suggest that in hearing animals, the density of prestin in the basolateral walls of apical and basal hair cells is the same. This conclusion differs somewhat from the findings of Santos-Sacchi *et al.*, (1998) where prestin density was assayed from non-linear capacitance measurements. These indicated that OHCs from high frequency regions of the guinea pig cochlea have a considerably higher density (≈ 9 -fold) of the motor protein in their basolateral membrane than lowest frequency regions. To examine this discrepancy, we also performed non-linear capacitance measurements on OHCs of hearing rats. The results were consistent with the immunolabelling and indicated no significant difference in prestin density between the same cochlear locations examined with labelling. The non-linear capacitance of OHCs may be influenced by a variety of treatments (e.g., phosphorylation or turgor pressure) but the primary consequence of these treatments is one of shifting the operating range or $V_{0.5}$, rather than altering the maximum charge density (Frolenkov, 2006). Furthermore, there is no evidence that such effects would differ systematically between apical and basal cells. An increase in charge density has been reported following chronic salicylate administration, but the change was less than 20 percent (Yu *et al.*, 2008).

One possible explanation for the discrepancy between the present conclusions and those of Santos-Sacchi et al., (1998) resides with the assumption used to derive the lateral membrane area in which the prestin is confined. In the earlier calculation (Santos-Sacchi et al., 1998), a constant area, $620 \mu\text{m}^2$, was subtracted from the total membrane area inferred from the linear capacitance to exclude the top and bottom aspects of the cell that are devoid of prestin. In our calculations, which were based explicitly on cellular dimensions, the excluded area is considerably less and moreover differs between low-frequency and high-frequency OHCs because of a smaller cell diameter and hair bundle in high frequency cells. The difference between total and lateral membrane area in our calculations was $318 \mu\text{m}^2$ and $207 \mu\text{m}^2$ in low- and high-frequency OHCs respectively. The large and fixed areal correction in Santos-Sacchi *et al.*, (1998) is likely to over-estimate the charge density especially in the smaller high-frequency OHCs where the correction constitutes a larger fraction of the total area.

It might be argued that immunolabelling targets all prestin molecules and does not distinguish between active and non-active forms whereas an active form might require attachment to other membrane proteins or cytoskeletal elements. However, if it is assumed that non-linear capacitance is an indicator of functionality, then the non-linear capacitance results reinforce the conclusion of a similar density of functional prestin in apical and basal OHCs. The two locations assayed in our experiments ($d = 0.8$ and $d = 0.3$) correspond to characteristic frequencies of 4 and 30 kHz respectively and do not represent the full auditory range of the rat which extends from 1 kHz to 60 kHz (Müller, 1991). Nevertheless, if there were a significant increase in prestin density along the tonotopic axis, some indication of this gradient should have been evident in the current measurements.

Maximum prestin density

In addition to the immunolabelling and non-linear capacitance data, a third method has been previously used to reveal the structure of the OHC membrane. Freeze fracture of the basolateral membrane shows a dense array of intra-membranous particles 10 nm in diameter. The particle density increases in parallel with electromotility to attain a mature level at P16 (Souter *et al.*, 1995) of $2,500 - 5,700 \mu\text{m}^{-2}$ (Forge, 1991; Kalinec *et al.*, 1992; Santos-Sacchi *et al.*, 1998). It is tempting to identify the particles with prestin but their size is too large and density too small to correspond to single molecules. A clue to the difference is the recent work showing that prestin forms tetrameric assemblies similar in size to the intra-membranous particles (Zheng *et al.*, 2006; Mio *et al.*, 2008). If this is the case, the maximum charge densities achievable based on the largest reported particle densities could be no more than four times the particle density, $10,000 - 23,000 \text{e}^- \mu\text{m}^{-2}$, which may be compared with our measurements in basal OHCs of $\approx 10,000 \text{e}^- \mu\text{m}^{-2}$.

Force production in OHCs

In modelling the contribution of OHC somatic motility to cochlear mechanics, it is important to know the variation in force production with cochlear location. If it is assumed that OHCs from both low frequency and high frequency locations possess equal densities of prestin of the same isoform then their force production will be the same despite differences in cell length, L . Force production, F , can be approximated by

$$F = E_x A \Delta L / L \quad (3)$$

where E_x is the axial Young's modulus, A is the 'effective area' over which force is produced and ΔL is the change in length. The maximum fractional change in OHC length on prestin activation, $\Delta L/L$, is the strain and is a function of the prestin density. The same

prestin density implies the same strain provided the prestin isoform and its environment are identical. Direct measurements of force generation during OHC depolarization have shown that this is approximately correct (Hallworth, 1995; Iwasa & Adachi, 1997). These measurements were made in guinea-pig OHCs from a range of cochlear positions as inferred from differences in maximum cell length L . In fact, the results suggested a small correlation with L so that force production increased two- to three-fold for a comparable increase in L : longer apical OHCs produce *more* force. This change could be partly explained by small differences in 'effective area' (basal cells have smaller diameter) and in the 'effective length' over which shortening occurs; i.e., part of the cell below the nucleus does not contain prestin and therefore does not shorten (Hallworth, 1995). These two factors might account for up to a 50 per cent increase in force production in apical cells. Taken together with the present results, the conclusion is that the maximum force produced by OHC somatic contractility at the apex and base are not significantly different. Whether an increase in force production is needed in basal OHCs compared to apical ones is unclear but this force needs to overcome the local impedance of the basilar membrane, its stiffness, viscosity and mass. Both stiffness (Naidu & Mountain, 1998; Emadi *et al.*, 2004) and viscous force (due to its scaling with velocity) are likely to increase at the high-frequency compared to low-frequency end of the cochlea. Indeed, an increase in force production in high frequency OHCs is often invoked in cochlear modelling (Mammano & Nobili, 1993; Geisler, 1993; Lu *et al.*, 2006). For example, Mammano & Nobili (1993) assume that the OHC force production is proportional to basilar membrane stiffness, Geisler (1993) assumes it is proportional to characteristic frequency and Lu *et al.*, (2006) assume it increases more than 100-fold from apex to base. The present results indicate that this assumption is unwarranted. Further experiments and modelling will be needed to understand the comparative efficacy of OHC somatic contractility at the two ends of the cochlea.

Acknowledgments

This work was supported by National Institutes on Deafness and other Communication Disorders grant RO1 DC01362 and a grant from the University of Wisconsin Steenbock foundation to R.F. Dr D.N. Furness is thanked for his useful discussion of the TEM images.

References

- Ashmore J. Cochlear outer hair cell motility. *Physiol. Rev* 2008;88:173–210. [PubMed: 18195086]
- Belyantseva IA, Adler HJ, Curi R, Frolenkov GI, Kachar B. Expression and localization of prestin and the sugar transporter GLUT-5 during development of electromotility in cochlear outer hair cells. *J. Neurosci* 2000;20:RC116. [PubMed: 11125015]
- von Békésy, G. *Experiments in Hearing*. New York: McGraw Hill; 1960.
- Dallos P. The active cochlea. *J. Neurosci* 1992;12:4575–4585. [PubMed: 1464757]
- Dallos P, Evans BN. High-frequency outer hair cell motility: corrections and addendum. *Science* 1995;268:1420–1421. [PubMed: 7770765]
- Dallos P, Zheng J, Cheatham MA. Prestin and the cochlear amplifier. *J. Physiol. (Lond)* 2006;576:37–42. [PubMed: 16873410]
- Dallos P, Wu X, Cheatham MA, Gao J, Zheng J, Anderson CT, Jia S, Wang X, Cheng WH, Sengupta S, He DZ, Zuo J. Prestin-based outer hair cell motility is necessary for mammalian cochlear amplification. *Neuron* 2008;58:333–339. [PubMed: 18466744]
- Emadi G, Richter CP, Dallos P. Stiffness of the gerbil basilar membrane: radial and longitudinal variations. *J Neurophysiol* 2004;91:474–488. [PubMed: 14523077]
- Fettiplace R, Hackney CM. The sensory and motor roles of auditory hair cells. *Nature Rev. Neurosci* 2006;7:19–29. [PubMed: 16371947]
- Forge A. Structural features of the lateral walls in mammalian cochlear outer hair cells. *Cell Tissue Res* 1991;265:473–483. [PubMed: 1786594]

- Frolenkov GI. Regulation of electromotility in the cochlear outer hair cell. *J. Physiol. (Lond)* 2006;576:43–48. [PubMed: 16887876]
- Geisler CD. A realizable cochlear model using feedback from motile outer hair cells. *Hear. Res* 1993;68:253–262. [PubMed: 8407611]
- Gillis, KD. Techniques for membrane capacitance measurements. In: Sakmann, B.; Neher, E., editors. 'Single channel recording'. 2nd edition. New York: Plenum Press; 1995. p. 155-198.
- Hackney CM, Mahendrasingam S, Penn A, Fettiplace R. The concentrations of calcium buffering proteins in mammalian cochlear hair cells. *J. Neurosci* 2005;25:7867–7875. [PubMed: 16120789]
- Hallworth R. Passive compliance and active force generation in the guinea pig outer hair cell. *J Neurophysiol* 1995;74:2319–2328. [PubMed: 8747194]
- Housley GD, Ashmore JF. Ionic currents of outer hair cells isolated from the guinea-pig cochlea. *J Physiol* 1992;448:73–98. [PubMed: 1593487]
- Iwasa KH, Adachi M. Force generation in the outer hair cell of the cochlea. *Biophys. J* 1997;73:546–555. [PubMed: 9199816]
- Jensen-Smith H, Hallworth R. Lateral wall protein content mediates alterations in cochlear outer hair cell mechanics before and after hearing onset. *Cell Motil. Cytoskeleton* 2007;64:705–717. [PubMed: 17615570]
- Kalinec F, Holley MC, Iwasa KH, Lim DJ, Kachar B. A membrane-based force generation mechanism in auditory sensory cells. *Proc. Natl. Acad. Sci. USA* 1992;89:8671–8675. [PubMed: 1528879]
- Kennedy HJ, Evans MG, Crawford AC, Fettiplace R. Fast adaptation of mechano-electrical transducer channels in mammalian cochlear hair cells. *Nat. Neurosci* 2003;6:832–836. [PubMed: 12872124]
- Kennedy HJ, Evans MG, Crawford AC, Fettiplace R. Depolarization of cochlear outer hair cells evokes active hair bundle motion by two mechanisms. *J. Neurosci* 2006;26:2757–2766. [PubMed: 16525055]
- Legendre K, Safieddine S, Küssel-Andermann P, Petit C, El-Amraoui A. Alpha II-betaV spectrin bridges the plasma membrane and cortical lattice in the lateral wall of the auditory outer hair cells. *J. Cell. Sci* 2008;121:3347–3356. [PubMed: 18796539]
- Lieberman MC, Gao J, He DZ, Wu X, Jia S, Zuo J. Prestin is required for electromotility of the outer hair cell and for the cochlear amplifier. *Nature* 2002;419:300–304. [PubMed: 12239568]
- Liu XZ, Ouyang XM, Xia XJ, Zheng J, Pandya A, Li F, Du LL, Welch KO, Petit C, Smith RJ, Webb BT, Yan D, Arnos KS, Corey D, Dallos P, Nance WE, Chen ZY. Prestin, a cochlear motor protein, is defective in non-syndromic hearing loss. *Hum. Mol. Genet* 2003;12:1155–1162. [PubMed: 12719379]
- Lu TK, Zhak S, Dallos P, Sarpeshkar R. Fast cochlear amplification with slow outer hair cells. *Hear. Res* 2006;214:45–67. [PubMed: 16603325]
- Mammano F, Ashmore JF. Differential expression of outer hair cell potassium currents in the isolated cochlea of the guinea-pig. *J Physiol* 1996;496:639–646. [PubMed: 8930832]
- Mammano F, Nobili R. Biophysics of the cochlea: linear approximation. *J. Acoust. Soc. Am* 1993;93:3320–3332. [PubMed: 8326060]
- Matsuda K, Zheng J, Du G, Klöcker N, Madison LD, Dallos P. N-linked glycosylation sites of the motor protein prestin: effects on membrane targeting and electrophysiological function. *J. Neurochem* 2004;89:928–938. [PubMed: 15140192]
- Mio K, Kubo Y, Ogura T, Yamamoto T, Arisaka F, Sato C. The motor protein prestin is a bullet-shaped molecule with inner cavities. *J. Biol. Chem* 2008;283:1137–1145. [PubMed: 17998209]
- Mistrík P, Mullaley C, Mammano F, Ashmore J. Three-dimensional current flow in a large-scale model of the cochlea and the mechanism of amplification of sound. *J. Roy. Soc. Interface* 2009;6:279–291. [PubMed: 18682366]
- Müller M. Frequency representation in the rat cochlea. *Hear. Res* 1991;51:247–254. [PubMed: 2032960]
- Naidu RC, Mountain DC. Measurements of the stiffness map challenge a basic tenet of cochlear theories. *Hear. Res* 1998;124:124–131. [PubMed: 9822910]

- Oliver D, Fakler B. Expression density and functional characteristics of the outer hair cell motor protein are regulated during postnatal development in rat. *J Physiol* 1999;519:791–800. [PubMed: 10457091]
- Preyer S, Renz S, Hemmert W, Zenner H-P, Gummer AW. Receptor potential of outer hair cells of the adult guinea pig cochlea: implications for cochlear tuning mechanisms. *Aud. Neurosci* 1996;2:145–157.
- Ramamoorthy S, Deo NV, Grosh K. A mechano-electro-acoustical model for the cochlea: response to acoustic stimuli. *J. Acoust. Soc. Am* 2007;121:2758–2773. [PubMed: 17550176]
- Robbins J. KCNQ potassium channels: physiology, pathophysiology and pharmacology. *Pharmacol. Ther* 2001;90:1–19. [PubMed: 11448722]
- Rybalchenko V, Santos-Sacchi J. Cl⁻ flux through a non-selective, stretch-sensitive conductance influences the outer hair cell motor of the guinea-pig. *J Physiol* 2003;547:873–891. [PubMed: 12562920]
- Santos-Sacchi J. Reversible inhibition of voltage-dependent outer hair cell motility and capacitance. *J. Neurosci* 1991;11:3096–3110. [PubMed: 1941076]
- Santos-Sacchi J. On the frequency limit and phase of outer hair cell motility: effects of the membrane filter. *J. Neurosci* 1992;12:1906–1916. [PubMed: 1578277]
- Santos-Sacchi J, Kakehata S, Kikuchi T, Katori Y, Takasaka T. Density of motility-related charge in the outer hair cell of the guinea pig is inversely related to best frequency. *Neurosci. Lett* 1998;256:155–158. [PubMed: 9855363]
- Santos-Sacchi J, Kakehata S, Takahashi S. Effects of membrane potential on the voltage dependence of motility-related charge in outer hair cells of the guinea-pig. *J Physiol* 1998b;510:225–235. [PubMed: 9625879]
- Souter M, Nevill G, Forge A. Postnatal development of membrane specialisations of gerbil outer hair cells. *Hear. Res* 1995;91:43–62. [PubMed: 8647724]
- Tunstall MJ, Gale JE, Ashmore JF. Action of salicylate on membrane capacitance of outer hair cells from the guinea-pig cochlea. *J Physiol* 1995;485:739–752. [PubMed: 7562613]
- Weitzel EK, Tasker R, Brownell WE. Outer hair cell piezoelectricity: frequency response enhancement and resonance behavior. *J. Acoust. Soc. Am* 2003;114:1462–1466. [PubMed: 14514199]
- Yu N, Zhu ML, Zhao HB. Prestin is expressed on the whole outer hair cell basolateral surface. *Brain Res* 2006;1095:51–58. [PubMed: 16709400]
- Yu N, Zhu ML, Johnson B, Liu YP, Jones RO, Zhao HB. Prestin up-regulation in chronic salicylate (aspirin) administration: an implication of functional dependence of prestin expression. *Cell. Mol. Life Sci* 2008;65:2407–2418. [PubMed: 18560754]
- Zheng J, Shen W, He DZ, Long KB, Madison LD, Dallos P. Prestin is the motor protein of cochlear outer hair cells. *Nature* 2000;405:149–155. [PubMed: 10821263]
- Zheng J, Du GG, Anderson CT, Keller JP, Orem A, Dallos P, Cheatham M. Analysis of the oligomeric structure of the motor protein prestin. *J. Biol. Chem* 2006;281:19916–19924. [PubMed: 16682411]

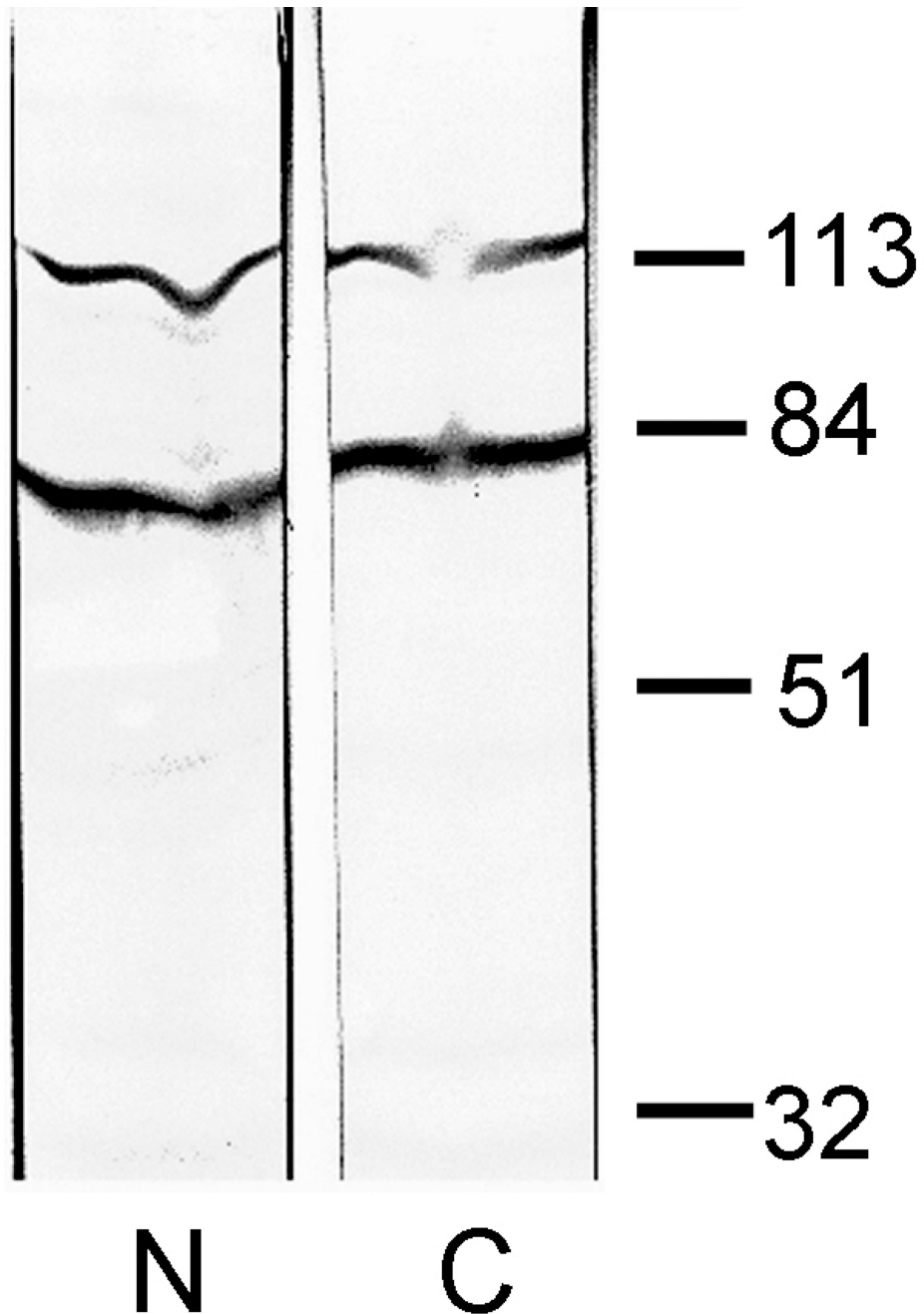


FIG. 1. Immunoblots of rat organ of Corti showing performance of anti-prestin antibodies

In the left-hand lane, the blot was labelled with the N-terminal antibody (N) at a dilution of 1:100 and in the right hand lane it was labelled with the C-terminal antibody (C) at a dilution of 1:25,000. Numbers to right give molecular weight markers in kDa. A principal band at 80 kDa corresponds to the molecular weight of rat prestin. The higher band at ~112 kDa may indicate a glycosylated form of prestin.

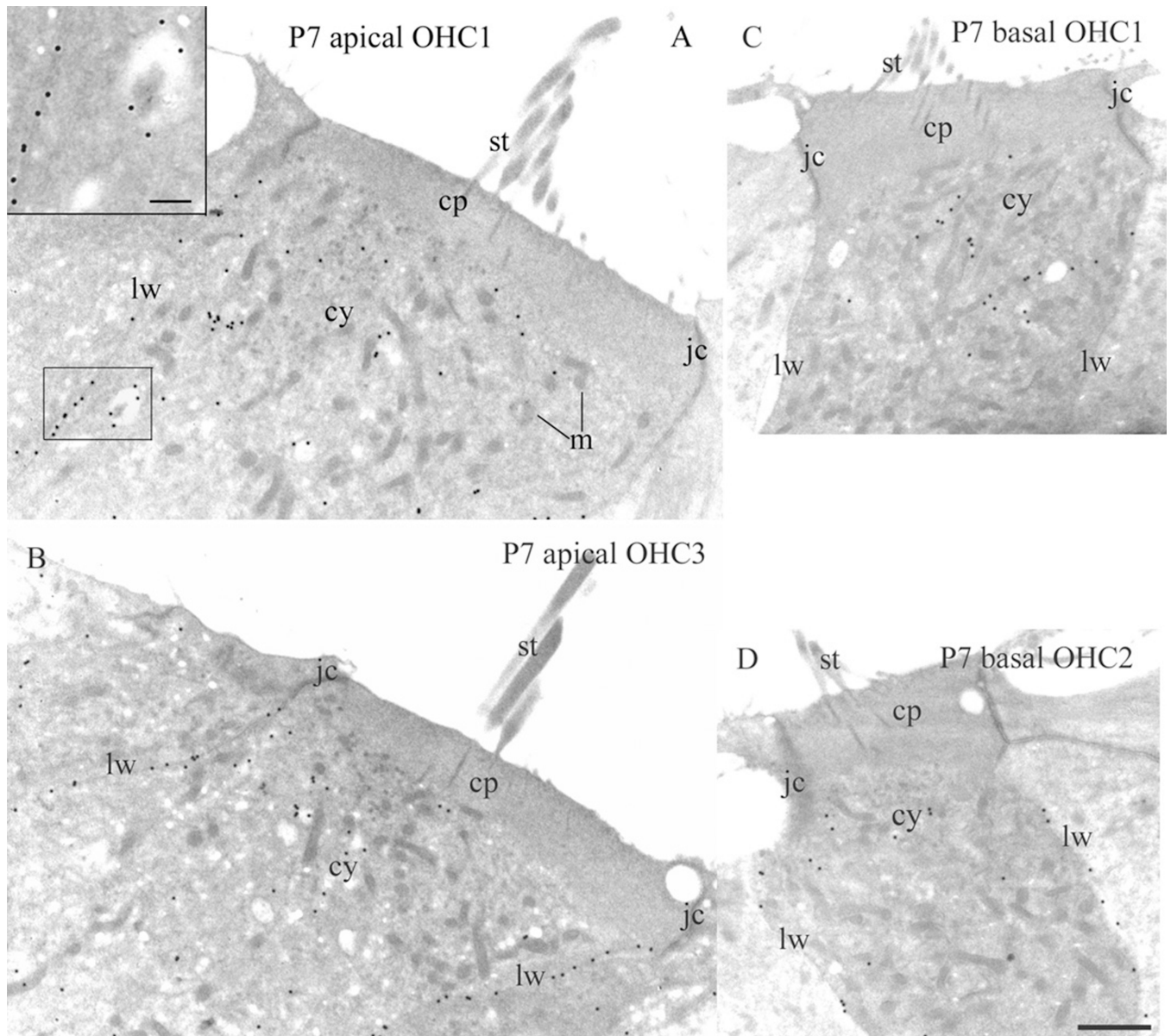


FIG. 2. Prestin labelling in apical and basal OHCs from P7 rats

Radial sections of apical OHC1 (A) and apical OHC3 (B) from a P7 rat immunogold labelled for prestin. Gold particles are localized along the basolateral walls (lw) and cytoplasm (cy) of the OHCs (A,B); and the inset in (A) is an enlargement of the boxed area of the basolateral wall of the apical OHC1. Radial sections of basal OHC1 (C), OHC2 (D) from a P7 rat immunogold labelled for prestin. Although several gold particles are localized on the basolateral walls (lw) of OHC2(D), only a few are localized on the basolateral wall(lw) of OHC1 (C). Gold particles are also localized in the cytoplasm (cy) of the OHCs, but not in their stereocilia (st), cuticular plate (cp), mitochondria (m) and junctions (jc). There are more gold particles on the basolateral wall of apical OHCs (A, B) than the basal ones (C, D). Scale bar = 1200 nm for (A) and (B), 1000 nm for (C) and (D) and 200 nm for the inset in (A). Note in all sections, except the inset in (A), gold particles have been enlarged (2.5 ×) for better visualization. Prestin antibody diluted 1:50,000.

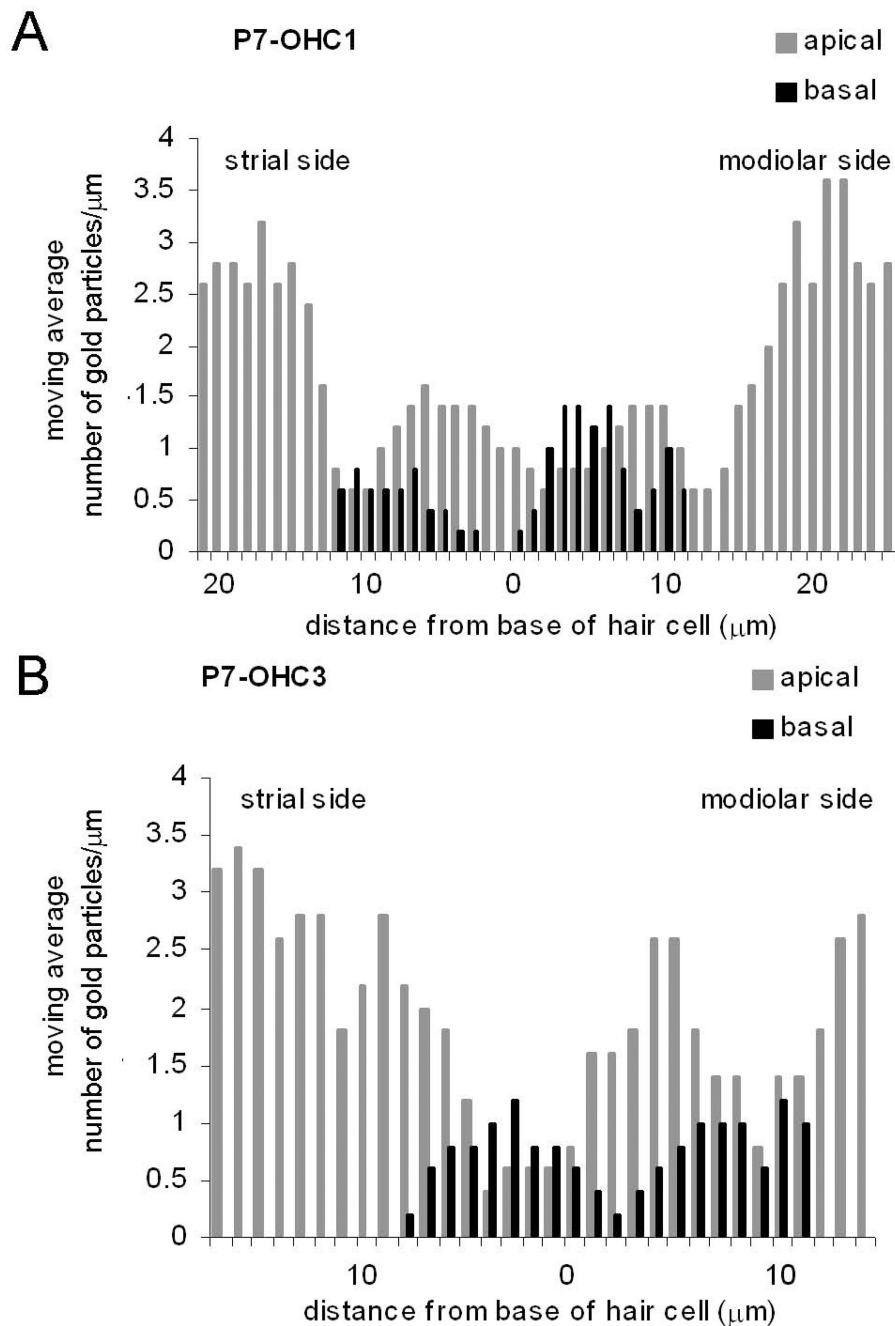


FIG. 3. Prestin distribution in a P7 rat

A. Bar plot showing distribution of immunogold labelling for prestin (antibody diluted 1:50,000) along the basolateral walls of apical and basal OHC1. B. Bar plot showing distribution of immunogold prestin labelling (antibody diluted 1:50,000) along the basolateral walls of apical and basal OHC3 from a P7 rat. Each bar is the moving average of counts. μm^{-1} averaged over 5 μm lengths of basolateral membrane, starting from the tight junction on the stria vascular aspect of the cell and proceeding along the membrane toward the bottom of the cell and then up the modiolar side. In (A) and (B), apical and basal plots are overlaid and both referenced to the bottom of the cell which is the zero point on the abscissa.

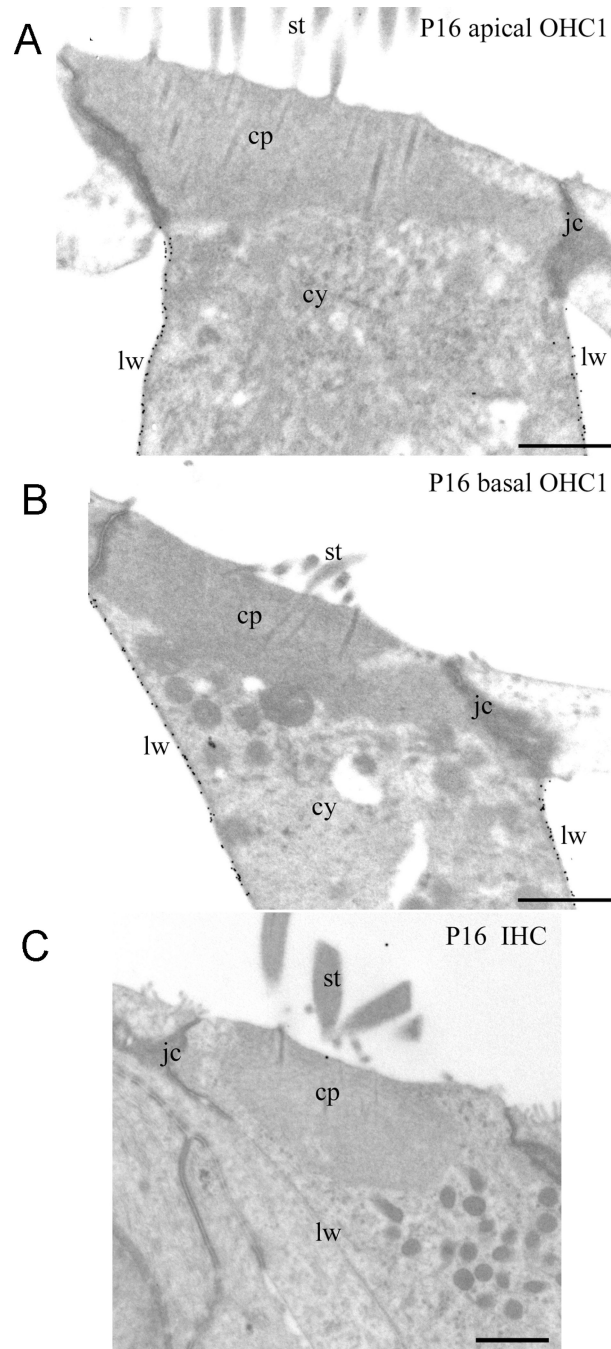


FIG. 4. Prestin labelling in apical and basal hair cells from a P16 rat

Radial sections of OHC1 (A and B) and IHC (C) from a P16 rat immunogold labelled for prestin (antibody diluted 1:50,000). Gold particles are localized on the basolateral walls (lw) of the OHC1 (A and B), and the labelling for prestin appears to be similar in the apical (A) and basal (B) OHC1; the stereocilia (st), cuticular plate (cp), cytoplasm (cy) and the junctions (jc) are not labelled for prestin. Note that no gold particles are localized in the IHC (C). Scale bars, 1 μ m.

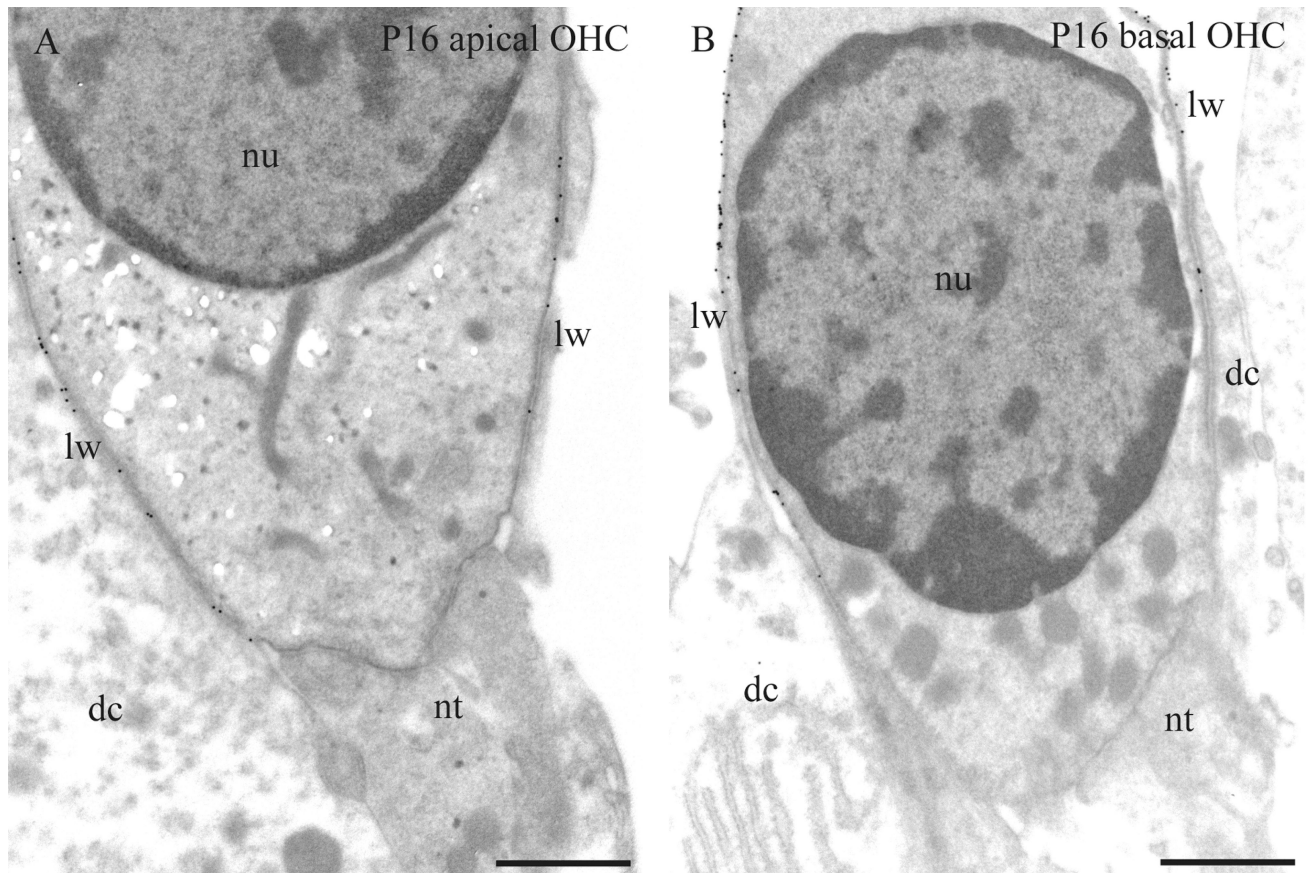


FIG. 5. Prestin labelling in the nuclear region of apical and basal OHCs

Radial sections of OHC from a P16 rat; apical (A) and basal (B) OHCs are immunogold labelled for prestin (antibody diluted 1:50,000). In the apical OHC (A), gold particles are localized in the entire length of the basolateral wall (lw) including the region below the nucleus (nu), except the region where nerve terminals (nt) contact the base of the hair cell. In the basal OHC (B) gold particles are localized on the basolateral wall (lw) up to the end of the level of nucleus (nu), and hardly any gold particle is localized below the level of the nucleus (nu); nerve terminals (nt); Deiters' cell (dc). Scale bars = 1 µm.

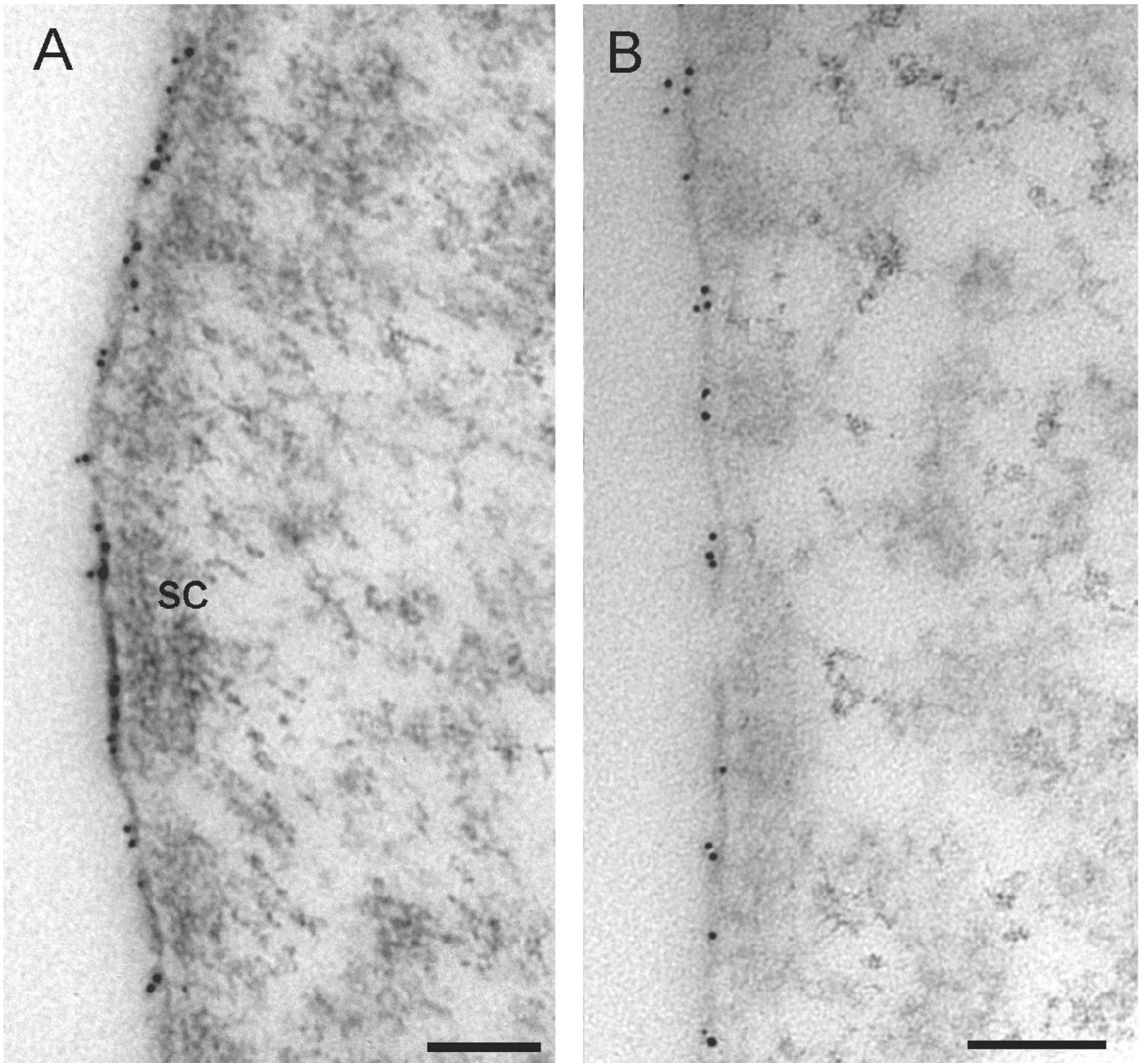


FIG. 6. Prestin localization to the plasma membrane

Radial sections of OHCs of a P16 rat labelled with primary antibodies to the prestin C-terminus (A) and N-terminus (B) and with a secondary antibody coupled to 5 nm gold particles. Note the immunogold is confined to the plasma membrane and there is none over the sub-membranous cisterna (sc). Scale bar 100 nm.

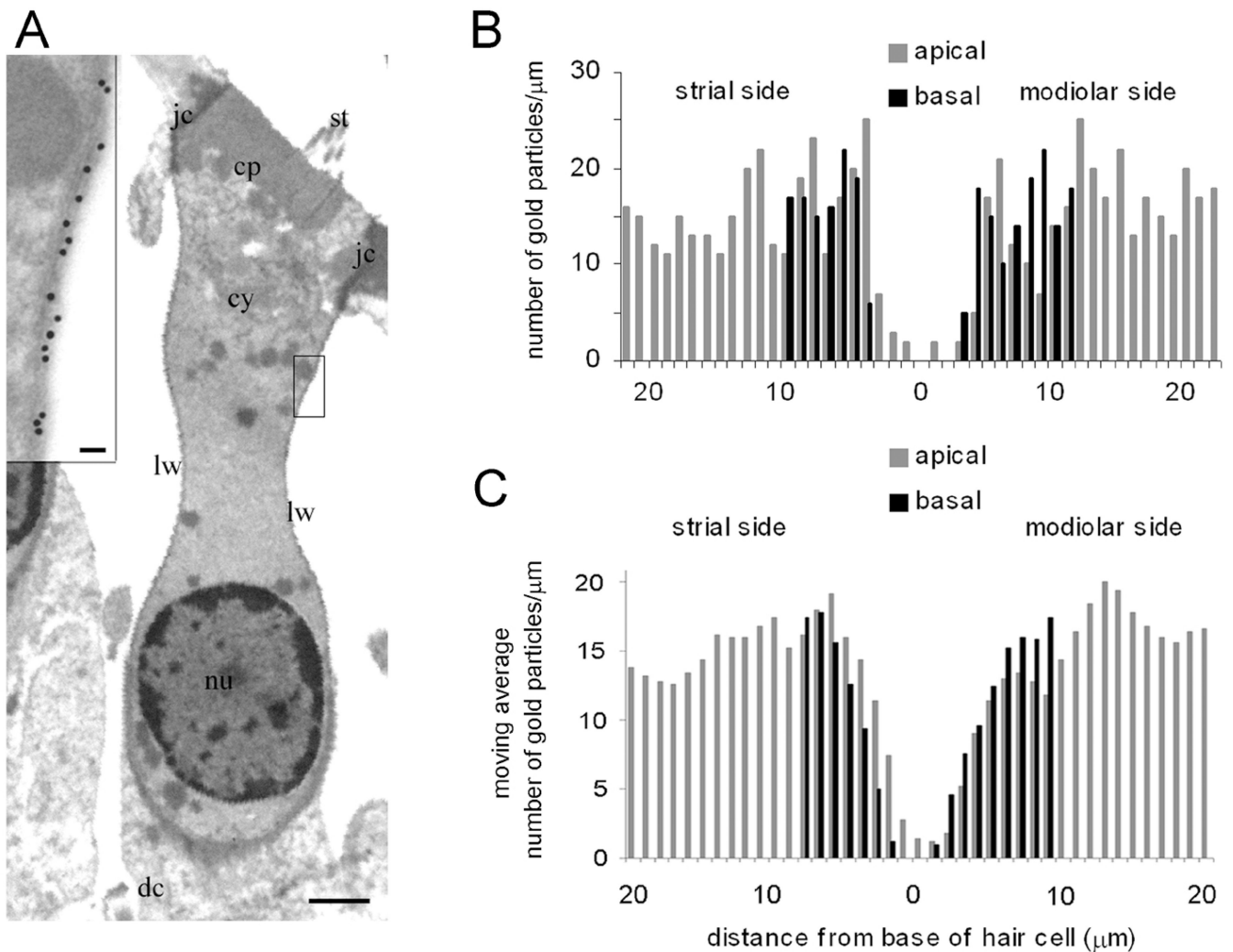


FIG. 7. Prestin distribution in a P16 rat

A. Radial section of a basal OHC2 immunogold labelled for prestin (antibody diluted 1:25,000). Gold particles are localized along the basolateral wall (lw) and the boxed area is enlarged in the inset (inset scale bar = 100 nm). Stereocilia (st), cuticular plate (cp), junctions (jc), cytoplasm (cy), nucleus (nu), Deiter's cell (dc). Scale bar = 1 μm . B. Bar plot showing distribution of immunogold labelling for prestin (antibody diluted 1:25,000) along the basolateral walls of apical OHC3 and basal OHC2 (same cell as in A) from a P16 rat. Each bar is the number of gold particle μm^{-1} from the tight junction on the stria vascular aspect of the cell along the membrane toward the bottom of the cell and then up the modiolar side. C. Bar plot showing the moving average of counts, μm^{-1} averaged over 5 μm lengths of basolateral membrane, from the tight junction on the stria vascular aspect of the cell along the membrane toward the bottom of the cell and then up the modiolar side. Apical and basal plots are overlaid and both referenced to the bottom of the cell which is the zero point on the abscissa. Note the absence of prestin labelling around the bottom of the cell, more evident in (B) than in the (C) where the moving average smoothing decreases spatial resolution.

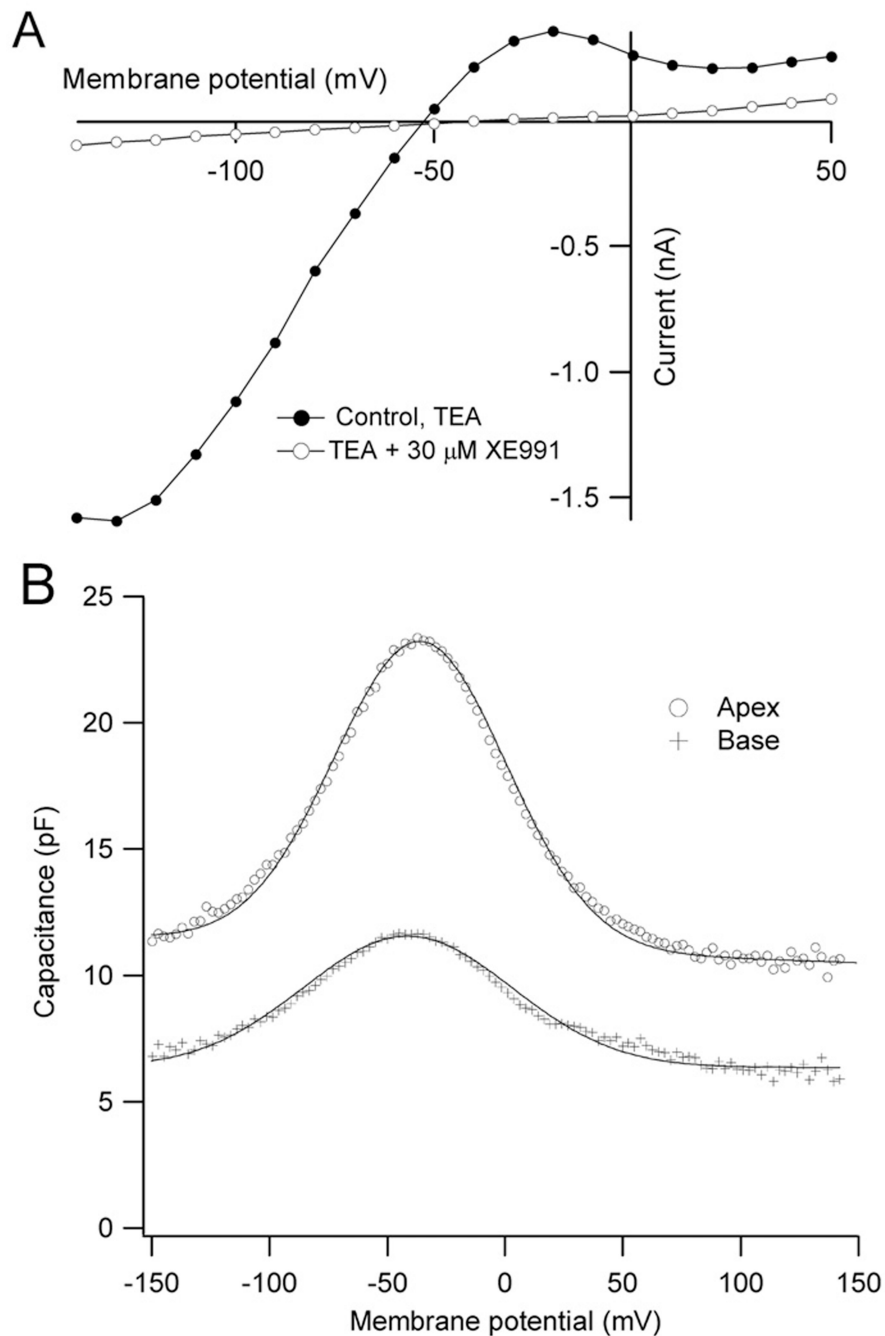


FIG. 8. Non-linear capacitance in apical and basal OHCs

A. Effects of blockers on the steady-state current voltage relationship of a basal OHC. When recorded with Cs^+ -based intracellular solution in the presence of 10 mM TEA outside, the OHC still showed a significant inward and outward current at negative membrane potentials. This was completely blocked by 30 μM XE991, an inhibitor of KCNQ channels, after which the input resistance was $> 1\text{G}\Omega$. B. Non-linear capacitance in an apical OHC (\circ) from a P18 rat and basal OHC (+) from a P16 rat. Measurements made in the presence of 10 mM TEA and 30 μM XE991 in the extracellular solution. Smooth curves are fits based on eqn. (1) with values of C_{LIN} , Q_{MAX} , $V_{0.5}$ and z of: 11 pF, 1.35 pC, -36 mV, 0.97 (apex) and 6.4 pF, 0.6 pC, -41 mV, 0.94 (base).

TABLE 1

Density of prestin immunolabelling in apical and basal OHCs of P16 rats

Cochlear region	d	CF (kHz)	OHC1 (μm^{-1})	OHC2 (μm^{-1})	OHC3 (μm^{-1})	Sample length (μm)
Apical	0.8	4	20.3 \pm 3.9 (3)	23.1 \pm 3.6 (3)	22.9 \pm 0.9 (5)	21.0 \pm 9.6 (11)
Basal	0.3	30	24.4 \pm 5.4 (5)	22.4 \pm 4.1 (5)	24.3 \pm 1.2 (4)	6.8 \pm 3.3 (14)

Mean density of gold particles per μm (\pm SD) along the basolateral membrane of the first, second and third row OHCs in the apical ($d = 0.8$) and basal ($d = 0.3$) regions of the rat cochlea. Numbers of cells are indicated in brackets. d is the fractional distance along the cochlea from the round window and CF is the characteristic frequency of the location from the tonotopic map of Müller (1991). For each cell, counts were made down a sample length of membrane above the nucleus whose mean and SD are given in last column. The sample length is larger at the apex because the cells are longer.

TABLE 2

Parameters derived from fits to OHC non-linear capacitance

d	CF (kHz)	Valence z	$V_{0.5}$ (mV)	Q ($e^- \cdot \mu\text{m}^{-2}$)	Q' ($e^- \cdot \mu\text{m}^{-2}$)	C_{LIN} (pF)	N
0.8	4	0.95 ± 0.05	-38 ± 3	6987 ± 559	9473 ± 758	12.1 ± 1.0	35
0.3	30	0.91 ± 0.06	-42 ± 3	6146 ± 926	9966 ± 1466	5.4 ± 0.7	11

Measurements \pm SD on P16 – P18 OHCs from the apex ($d = 0.8$) and P14 – P16 OHCs from base ($d = 0.3$). Parameters obtained from fitting eqn. (1): z (slope), $V_{0.5}$ (membrane potential for half-activation), C_{LIN} (linear capacitance) and Q (charge density). Q was obtained by scaling Q_{max} (the maximum nonlinear charge moved) by the total OHC membrane area calculated from the linear capacitance assuming a specific membrane capacitance of $0.01 \text{ pF} \cdot \mu\text{m}^{-2}$. Q' was calculated from Q_{max} using OHC dimensions assuming the prestin was confined to the lateral wall from the cell apex to the middle of the nucleus (see text). d is the fractional distance along the cochlea from the round window and CF is the characteristic frequency of the location from the tonotopic map of Müller (1991).